Dynamics of position-disordered Ising spins with a soft-core potential

Canzhu Tan,[1,2] Xiaodong Lin,[1,2] Yabing Zhou,[1,2] Yuhai Jiang,[3,2] Matthias Weidemüller,[1,2,4] and Bing Zhu[4,2,*]

[1]*Hefei National Laboratory for Physical Sciences at the Microscale and Shanghai Branch, University of Science and Technology of China, Shanghai 201315, China*

[2]*CAS Center for Excellence and Synergetic Innovation Center in Quantum Information and Quantum Physics, University of Science and Technology of China, Shanghai 201315, China*

[3]*Center for Transformative Science and School of Physical Science and Technology, ShanghaiTech University, Shanghai 201210, China*

[4]*Physikalisches Institut, Universität Heidelberg, Im Neuenheimer Feld 226, 69120 Heidelberg, Germany*

(Received 31 October 2021; revised 18 January 2022; accepted 9 March 2022; published 23 March 2022)

We theoretically study the magnetization relaxation of Ising spins distributed randomly in a d-dimension homogeneous and Gaussian profile under a soft-core two-body interaction potential $\propto 1/[1+(r/R_c)^\alpha]$ ($\alpha \geqslant d$), where r is the interspin distance and R_c is the soft-core radius. The dynamics starts with all spins polarized in the transverse direction. In the homogeneous case, an analytic expression is derived at the thermodynamic limit, which starts as $\propto \exp(-kt^2)$ with a constant k and follows a stretched-exponential law at long time with an exponent $\beta = d/\alpha$. In between an oscillating behavior is observed with a damping amplitude. For Gaussian samples, the degree of disorder in the system can be controlled by the ratio l_ρ/R_c, with l_ρ the mean interspin distance and the magnetization dynamics is investigated numerically. In the limit of $l_\rho/R_c \ll 1$, a coherent many-body dynamics is recovered for the total magnetization despite the position disorder of spins. In the opposite limit of $l_\rho/R_c \gg 1$, a similar dynamics as that in the homogeneous case emerges at a later time after a initial fast decay of the magnetization. We obtain a stretched exponent of $\beta \approx 0.18$ for the asymptotic evolution with $d = 3, \alpha = 6$, which is different from that in the homogeneous case ($\beta = 0.5$).

DOI: 10.1103/PhysRevB.105.104204

I. INTRODUCTION

Disorder plays an essential role in determining both equilibrium and nonequilibrium properties of a many-body system, e.g., glassy phase and dynamics in spin glasses [1], localization phenomenon of transports [2], and novel materials by disorder engineering [3–5]. While knowing microscopic details of a disordered system is difficult and not necessary, understanding its universal behavior, starting from a microscopic Hamiltonian, is important to pin down the underlying physics. For example, many relaxations in glassy materials (normal or spin type) follow a simple stretched-exponential law ($\propto \exp[-(\gamma t)^\beta], \beta < 1$) [1,6]. Klafter and Shlesinger found that a scale-invariant distribution of relaxation times was the common underlying structure for three different physical models showing a stretched-exponential decay [7], which was generalized to closed quantum systems by Schultzen and co-workers recently [8] (see also relevant phenomena in classical spin systems [9]).

For a disordered spin-1/2 system, recent studies confirmed a stretched-exponential decay of magnetization in both Ising [8] and Heisenberg [10,11] models, where the pairwise spin-spin interaction exhibits a power-law dependence on the interspin distance r, $J(r) \propto 1/r^\alpha$ with $\alpha \geqslant d$ in the d dimensions. The scale invariance is guaranteed, since a pairwise contribution to the relaxation dynamics is determined by $J(r)t$, which is invariant under the following rescaling of space and time: $r \to \lambda r$ and $t \to \lambda^\alpha t$.

In this work we consider a specific type of pairwise interactions in an Ising Hamiltonian, namely, a soft-core potential $J(r) \propto 1/[1+(r/R_c)^\alpha]$ with $\alpha \geqslant d$ and R_c the soft-core radius, reducing to the power-law behavior at large r. Soft-core potentials explicitly break the spatial scale invariance and have been investigated a lot in both classical [12–14] and quantum [15–23] regimes, focusing on the formation of particle clusters and crystals. Recently, it was shown that particles interacting via soft-core potentials in one dimension can feature an Ising criticality for both quantum [21] and classical [24] systems. The specific form of soft-core potential considered here is most relevant to Rydberg dressing in cold-atom experiments, where various spin models have been investigated both experimentally [25–29] and theoretically [30–33]. Moreover, we will show that the degree of interaction disorder with the considered soft-core potential can be tuned from a fully ordered case to a strongly disordered one via tuning the effective size of an inhomogeneously distributed spin sample, which is now experimentally feasible [34].

Here we have studied two different situations for Ising spins interacting via the soft-core potential: (i) For homogeneously distributed spins, an analytical formula is derived for the magnetization relaxation at the thermodynamic limit, which features three different regions in the time axis: the dynamics starts as $\propto \exp(-kt^2)$, followed by an oscillating decay, and eventually obeys a stretched-exponential law.

*bzhu@physi.uni-heidelberg.de

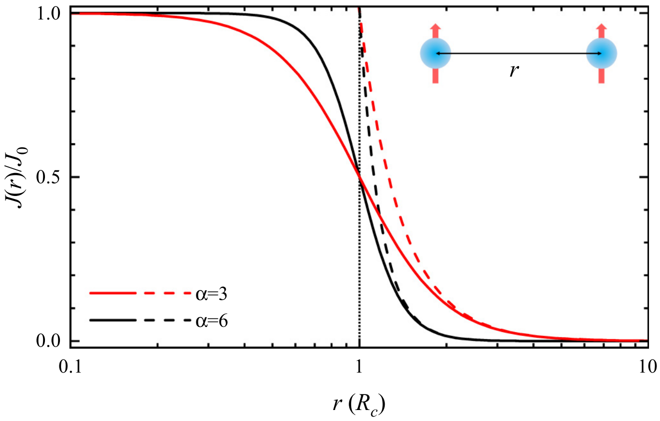

FIG. 1. Soft-core interaction potential between two spin-up particles. The soft-core potential in Eq. (2) is plotted as a function of interspin distance r with $\alpha = 3$ and 6 (solid curves). As a comparison, the power-law interactions $J_0/(r/R_c)^\alpha$ are also shown.

(ii) For a spatially inhomogeneous sample, e.g., Gaussian distributed, we observe the crossover from a fully ordered dynamics to a disorder-dominated one by changing the size of the spatial distribution of spins. A coherent many-body dynamics is observed in a small-spatial-size system, while disorder-induced relaxation is recovered for large spatial sizes.

The article is organized as follows: We derive and discuss the analytical result for homogeneous samples in Sec. II B. The inhomogeneous situation is numerically investigated in Sec. II C, and Sec. III concludes the paper.

II. DISORDERED ISING MODEL WITH A SOFT-CORE POTENTIAL

A. The Ising Hamiltonian and its dynamics

A general Ising Hamiltonian for N spin-1/2 particles reads

$$\hat{H}_{\text{Ising}} = \frac{1}{2}\sum_{i,j}^{N} J_{ij}\hat{\sigma}_i^z\hat{\sigma}_j^z, \tag{1}$$

where $\hat{\sigma}^z_{i(j)}$ is the Pauli z operator and J_{ij} is the coupling strength between spins i and j. J_{ij} takes a form of the soft-core potential

$$J_{ij} \equiv J(r_{ij}) = \frac{J_0}{1 + \left(\frac{r_{ij}}{R_c}\right)^\alpha}, \tag{2}$$

where the long-range part ($r_{ij} \gg R_c$) has a power-law form ($\propto 1/r_{ij}^\alpha$) and the short-range ($r_{ij} \ll R_c$) interaction is almost a constant J_0, as seen in Fig. 1. Such a potential is not invariant under the spatial scaling $r \to \lambda r$ in general, while it is approximately invariant at large $r \gg R_c$. We will see later that this leads to a stretched-exponential relaxation for long-time dynamics, both in the analytic solution of a homogeneous sample and the numerical results of a Gaussian one.

We focus on dynamics of the mean magnetization $\langle\hat{S}_x(t)\rangle = \langle\sum_{i=0}^N \hat{\sigma}_x^i(t)\rangle/N$ with an initial state that all spins are polarized in the $+x$ direction $|\phi_0\rangle = |{\to}\rangle^{\otimes N}$ with $\hat{\sigma}_x|{\to}\rangle = +1|{\to}\rangle$, i.e., $\langle\hat{S}_x(0)\rangle = 1$. Emch [35] and Radin [36] have obtained an analytical expression for $\langle\hat{S}_x(t)\rangle$ with the initial state $|\phi_0\rangle$, which reads as

$$\langle\hat{S}_x(t)\rangle = \sum_{i=1}^{N} 1/N \prod_{j\neq i}\cos(J_{ij}t). \tag{3}$$

All following analytical and numerical results are based on the above equation.

B. Homogeneous samples: The thermodynamic limit

We consider a system of N spins uniformly distributed in a spherical volume V in the d dimensions. Following the same derivation procedure in Ref. [8], by replacing the ensemble average with an average over all possible configurations of placing $N-1$ spins around a reference one at $\mathbf{r}_1 = \mathbf{0}$, Eq. (3) can be transformed to

$$\begin{aligned}\langle\hat{S}_x(t)\rangle &= \int_V d\mathbf{r}_2\cdots d\mathbf{r}_N P(\mathbf{r}_2,\ldots,\mathbf{r}_N)\prod_{j=2}^{N}\cos(J_{1j}t)\\ &= \left\{\frac{1}{V}\int_V d\mathbf{r}\cos[J(r)t]\right\}^{N-1}\\ &= \left\{\frac{d}{r_0^d}\int_0^{r_0} r^{d-1}dr\cos\left[\frac{J_0t}{1+(r/R_c)^\alpha}\right]\right\}^{N-1}.\end{aligned} \tag{4}$$

Here $P(\mathbf{r}_2,\ldots,\mathbf{r}_N) = 1/V^{N-1}$ is the probability of placing the $N-1$ spins at positions $\mathbf{r}_2,\ldots,\mathbf{r}_N$, respectively, and $J(r)$ takes the form in Eq. (2).

For the power-law interaction ($\propto 1/r^\alpha$) a short-distance cutoff has to be introduced to avoid the divergence of interaction strength for further simplifying Eq. (4) [8], which is not necessary for the soft-core potential considered here. By introducing a new variable $y = J_0t/[1+(r/Rc)^\alpha]$ and integrating by parts, Eq. (4) can be written as

$$\langle\hat{S}_x(t)\rangle = \left[1 - \frac{\pi^{d/2}\rho R_c^d}{\Gamma(d/2+1)N}\int_{y_0}^{J_0t}(J_0t/y-1)^{\beta_0}\sin y\, dy\right]^{N-1}, \tag{5}$$

where $V = \pi^{d/2}r_0^d/\Gamma(d/2+1)$ is the volume in d dimensions with the radius r_0, $N = \rho V = \rho\pi^{d/2}r_0^d/\Gamma(d/2+1)$, $\beta_0 = d/\alpha$, and $y_0 = J_0t/[1+(r_0/Rc)^\alpha]$. Here ρ is the particle density and $\Gamma(x)$ is the Gamma function. In the thermodynamic limit ($N, r_0 \to \infty$ and ρ is a constant), the integral $I(J_0t;\beta_0) = \int_{y_0}^{J_0t}(J_0t/y-1)^{\beta_0}\sin y\, dy$ is finite only if $\beta_0 \leqslant 1$ and the above equation gives

$$\langle\hat{S}_x(t)\rangle = \exp[-fI(J_0t;\beta_0)] \quad , \tag{6}$$

where $f = \pi^{d/2}\rho R_c^d/\Gamma(d/2+1)$.

Let us first consider $\beta_0 = 1$,

$$I(J_0t;1) = J_0t\,\mathrm{Si}(J_0t) + \cos(J_0t) - 1, \tag{7a}$$

where $\mathrm{Si}(x) = \int_0^x \sin(t)/t\,dt$ is the sine integral function. At short times

$$(J_0t \ll 1), I(J_0t;1) \sim 1/2(J_0t)^2, \tag{7b}$$

while

$$I(J_0t;1) \sim \pi/2J_0t - 1 \tag{7c}$$

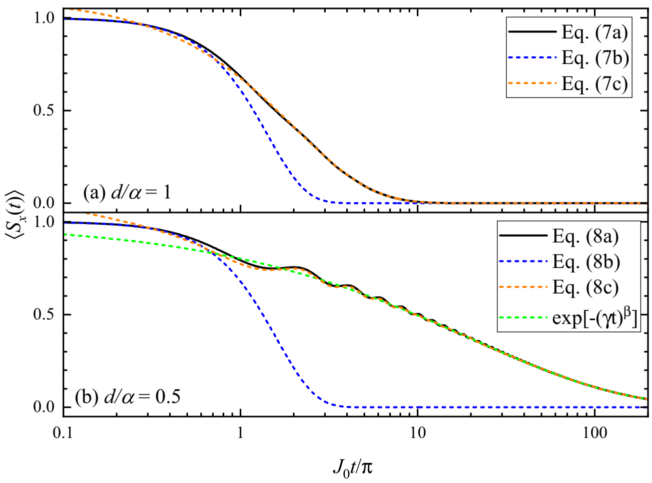

FIG. 2. Plots of analytic results for magnetization relaxation in uniformly distributed Ising spins under a pairwise soft-core interaction. (a) The case of $\beta_0 = d/\alpha = 1$. The black solid, blue dashed, and orange dashed curves represent the complete [Eq. (7a)], short-time asymptotic [Eq. (7b)], and long-time asymptotic [Eq. (7c)] expressions, respectively. (b) As in (a) for the case of $\beta_0 = d/\alpha = 0.5$. We also show the stretched-exponential function as a green curve for comparison.

for long times ($J_0t \gg 1$). In Fig. 2(a), all three formulas are plotted as a function of evolution time, and Eqs. (7b) and (7c) agree very well with the full solution Eq. (7a) concerning the asymptotic dynamics at short and long times, respectively. Specifically, a stretched-exponential decay, $\exp[-(\gamma t)^\beta]$ with $\beta = \beta_0 = 1$, $\gamma = J_0 f\pi/2$, is seen for the long-time dynamics.

Next we look at $\beta_0 < 1$. The integral $I(J_0t;\beta_0)$ is

$$I(J_0t;\beta_0) = J_0tB(1-\beta_0, 1+\beta_0)\Im[{}_1F_1(1-\beta_0, 2, iJ_0t)], \tag{8a}$$

where $B(x, y)$ is the Euler β function, ${}_1F_1(a, b, z)$ is the Kummer confluent hypergeometric function, and $\Im[z]$ gives the imaginary part of z. More details can be found in Appendix A 1. The asymptotic behaviors of Eq. (8a) are

$$I(J_0t;\beta_0) \sim 1/2(J_0t)^2(1-\beta_0)B(1-\beta_0, 1+\beta_0) \tag{8b}$$

for short times ($J_ot \ll 1$) and

$$\begin{aligned} I(J_0t;\beta_0) \sim (J_0t)^{\beta_0}[&\cos(\beta_0\pi/2)\Gamma(1-\beta_0) \\ &- (J_0t)^{-2\beta_0}\cos(J_0t-\beta_0\pi/2)\Gamma(1+\beta_0)] \end{aligned} \tag{8c}$$

for long times ($J_0t \gg 1$).

The asymptotic form of Eq. (8b) for $\beta_0 \to 1$ actually coincides with Eq. (7b). Thus, for $\beta_0 \leqslant 1$ the initial dynamics of $\langle\hat{S}_x(t)\rangle$ follows $\exp[-kt^2]$ with $k = J_0^2 f(1-\beta_0)B(1-\beta_0, 1+\beta_0)/2$. In the long-time limit, the second term inside the square bracket in Eq. (8c) can be neglected and the first term has an asymptotic value of $\pi/2$ for $\beta_0 \to 1$. So the long-time behavior of $\langle\hat{S}_x(t)\rangle$ is a stretched exponential $\exp[-(\gamma t)^\beta]$ with $\beta = \beta_0$ and $\gamma = J_0[f\cos(\beta_0\pi/2)\Gamma(1-\beta_0)]^{1/\beta_0}$. As a specific example, we show plots of Eq. (6) with $I(J_0t;\beta_0)$ from Eqs. (8a), (8b), and (8c) in Fig. 2(b) for $\beta_0 = 0.5$. Other than the two limits discussed before, a damped oscillating decay is observed in between, which to a large extent can be captured by the neglected second term inside the square bracket in Eq. (8c). This oscillating decay signatures the breakdown of scale invariance with the soft-core potential.

C. Gaussian samples: A numerical study

To extend the above analytic result for the homogeneous case, we numerically investigate the magnetization relaxation for an inhomogeneously distributed spin sample (Gaussian distributed) in this section, where the degree of disorder can be tuned. We focus on dynamics of the magnetization $\langle\hat{S}_x(t)\rangle$ under the setting specified in Sec. II A, however, with spin positions $\boldsymbol{r} = (x, y, z)$ randomly distributed in a three-dimension Gaussian distribution ($d = 3$),

$$G(\boldsymbol{r}) = \frac{1}{(2\pi)^{3/2}w_xw_yw_z}\exp\left(-\frac{x^2}{2w_x^2} - \frac{y^2}{2w_y^2} - \frac{z^2}{2w_z^2}\right), \tag{9}$$

where w_η is the standard deviation in η direction ($\eta \in \{x, y, z\}$). This distribution of spins could be realized with ultracold atoms trapped in harmonic traps [37]. The mean particle density is $\rho = N/(8\pi^{3/2}w_xw_yw_z)$ with the total particle number N, and for simplicity we assume $w_x = w_y = w_z \equiv w$, giving rise to a mean interspin distance of $l_\rho \equiv \rho^{-1/3} = 2\sqrt{\pi}w/N^{1/3}$ and its corresponding interaction strength $J_\rho = J(l_\rho) = J_0/[1 + (\pi^{d/2}/F\Gamma(d/2+1))^{1/\beta_0}]$ in Eq. (2), with F, β_0 defined in Sec. II B. For the following numeric calculation, we fix the total spin number $N = 100$ and $\alpha = 6$ ($\beta_0 = 0.5$).

For the soft-core potential in Eq. (2), R_c separates the interaction-strength randomness into two different regimes according to the ratio l_ρ/R_c for the above Gaussian sample. We show in Fig. 3 the distribution of pair interaction strengths with 100 spins randomly distributed according to Eq. (9) for three different values of l_ρ/R_c: 0.1, 1, and 5. When l_ρ is much smaller than R_c [$l_\rho/R_c = 0.1$ in Fig. 3(a)], $J(r)$ is almost the constant J_0 for all pairs, and hence randomness is minimized. Otherwise, when $l_\rho/R_c \gtrsim 1$ the distribution of $J(r)$ spans over several orders of magnitude, as seen in Figs. 3(b) and 3(c). Thus effects arising from disorder are expected to be important in this regime.

To explore the magnetization dynamics, we first randomly sample the positions of N spins according to the Gaussian distribution in Eq. (9) and evolve the system under Eq. (3) with the corresponding distribution of interaction strengths (see Fig. 3). We then repeat this random sampling for many times and obtain the spin magnetization at various times by averaging over the many realizations under the same parameters.

1. *High-density regime*

In Fig. 4 we present the numerical results from Eq. (3) for $l_\rho/R_c \in (0.1, 0.2)$ ($\rho \sim 10^{14} - 10^{15}$ cm^{-3} for $R_c = 1\,\mu$m), coined the *high-density regime*. In this regime the system behaves like an all-to-all interacting one with a single interaction strength J_0 [38], recovering a coherent many-body dynamics, as seen in Fig. 4(a) for the magnetization dynamics with $l_\rho/R_c = 0.1$. A fast initial decay of magnetization due to the

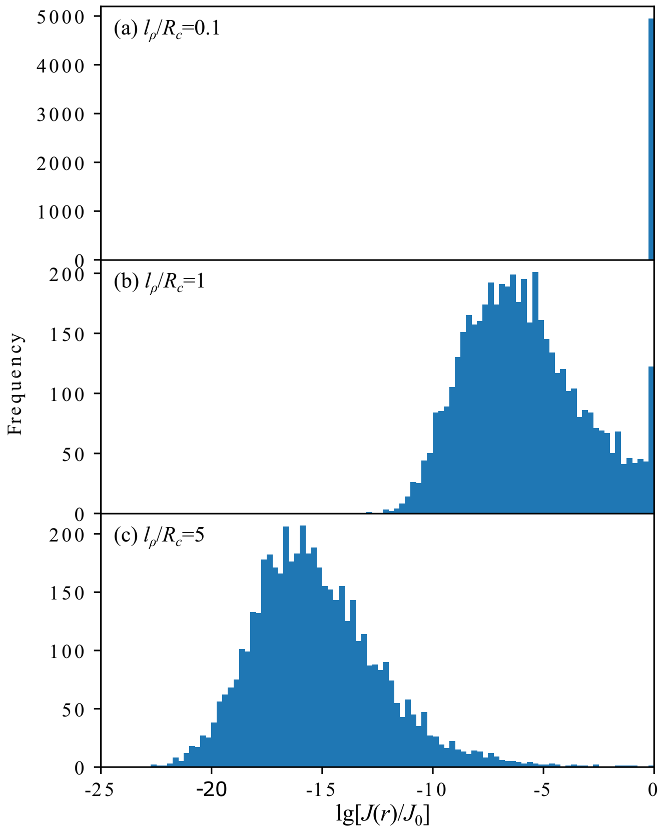

FIG. 3. Distribution of the pair interaction strength $J(r)$ for 100 spins randomly distributed in a three-dimensional Gaussian profile. (a), (b), (c) The distribution of $\lg[J(r)/J_0]$ for a mean interparticle distance of $l_\rho/R_c = 0.1$, 1, 5, respectively.

buildup of correlations [27,39] and periodic quantum revivals with decaying amplitudes are observed.

In Eq. (3), if all the interaction strengths take a common value of J_0, the resulting dynamics of $\langle \hat{S}_x(t)\rangle$ has an analytic form, $\langle \hat{S}_x(t)\rangle = \cos^{N-1}(J_0 t)$, giving rise to a coherent many-body quantum-revival dynamics [38]. To account for the observed decaying revival dynamics in Fig. 4(a), we phenomenologically fit the numerical data to a form of $\cos^{N-1}(J_0 t)\exp[-(\gamma_h t)^{\beta_h}]$, which is a stretched-exponential decay shown as the red curve in the figure. Note that we have tried fits with a pure exponential decay, which cannot fully capture the observed dynamics. From the fit we obtain the stretched exponents β_h and decay rates γ_h for various values of l_ρ/R_c, which are plotted in Fig. 4(b). We observe a monotonic approach to the normal exponential decay ($\beta_h = 1$) from $\beta_h > 1$ with an increasing disorder in the system (see Fig. 3), while the decay rate γ_h increases from 0 to the order of J_0.

2. Low-density regime

In the other regime with $l_\rho/R_c > 1$ ($\rho < 10^{12}$ cm^{-3} for $R_c = 1\,\mu$m), the pair interaction strengths distribute over a range covering 5 or 6 orders of magnitude (see Fig. 3). The results for dynamics of $\langle \hat{S}_x\rangle$ at six different values of l_ρ/R_c are shown in Fig. 5. As the cloud size w (l_ρ) increases, the initial collapse phase [see Fig. 4(a)] shrinks and a slow decay with

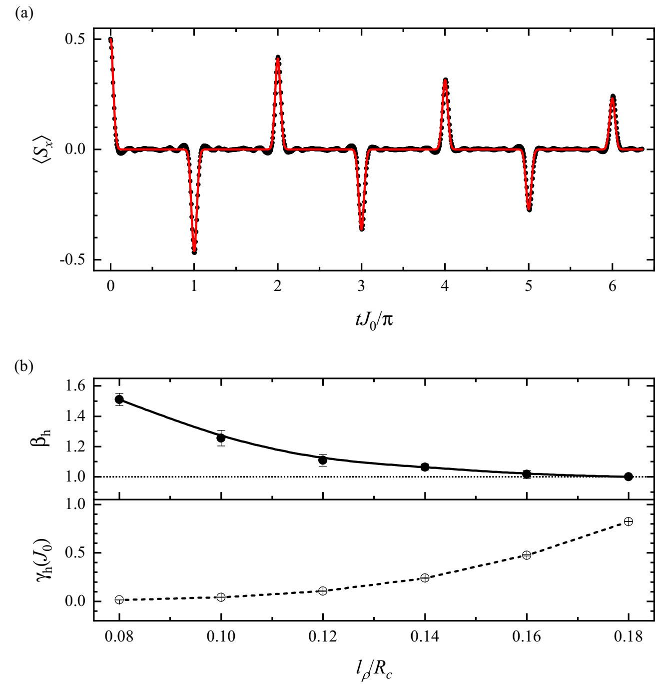

FIG. 4. Magnetization dynamics in a high-density Gaussian sample. (a) The time evolution of mean magnetization $\langle \hat{S}_x\rangle$ (solid points) for $l_\rho/R_c = 0.1$. After a initial fast decay, quantum revivals are observed with a damped amplitude. The red curve is a fit to the function of $\cos^{N-1}(J_0 t)\exp[-(\gamma_h t)^{\beta_h}]$ (see text for details), with which the stretched exponent β_h and decay rate γ_h are extracted. (c) The fitted β_h and γ_h as a function of l_ρ/R_c. The lines are guides to eyes. See text for more discussion.

an oscillating feature merges at long time, which is similar as that in Fig. 2(b).

We rescale the time t for each curve in Fig. 5 by the characteristic interaction strength J_ρ (as introduced in the beginning

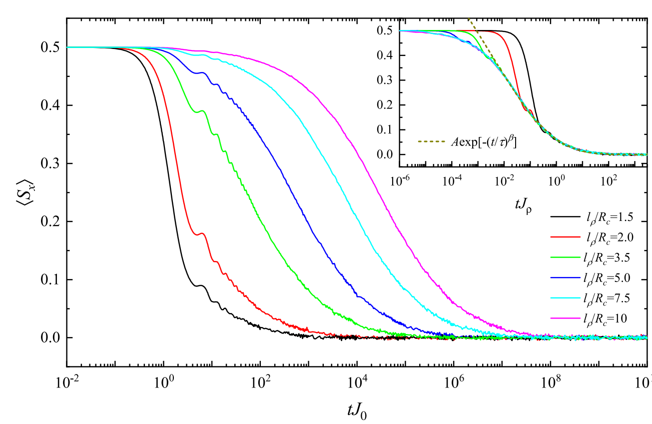

FIG. 5. Magnetization dynamics in a low-density Gaussian sample. Evolution curves of $\langle \hat{S}_x\rangle$ for six different values of l_ρ/R_c ranging from 1.5 to 10 are plotted. As l_ρ increases (ρ decreases), the initial fast decay seen in Fig. 4(a) shrinks along the time axis and a slow dynamics similar to that in Fig. 2 emerges. In the inset, the rescaled evolution curves ($tJ_0 \to tJ_\rho$) are shown, all of which fall onto a common one at the long-time part. We fit this common part to a stretched-exponential function (dashed dark yellow curve) and obtain an exponent of $\beta = 0.1817(9)$ and a decay rate of $\gamma = 343(15)J_\rho$.

of this section), which is presented in the inset. Curves for different l_ρ/R_c fall onto a common one at the long-time part, including the oscillation, which occupies a larger region in the dynamics for larger l_ρ/R_c and demonstrates a universal behavior. We fit this common long-time part of the $\langle \hat{S}_x \rangle$ dynamics to the stretched-exponential function $A\exp[-(\gamma t)^\beta]$ with the fitting parameter A, γ, β (dashed curves in the inset of Fig. 5). The fitted exponent β is 0.1817(9), and the decay rate γ is $343(15)J_\rho \approx 19.5(9)J_0F^{1/\beta_0}$ ($F \ll 1$). Both the stretched exponent and decay rate are different from the values obtained analytically for a homogeneous sample with $\beta_0 = 0.5$ in Sec. II B, where $\beta = \beta_0 = 0.5$, $\gamma \approx 1.57J_0F^{1/\beta_0}$.

III. CONCLUSION

In conclusion, we have considered magnetization relaxation of homogeneous and inhomogeneous samples of Ising spins with a soft-core pairwise potential. We have derived an analytic formula describing the whole dynamics in the homogeneous case, with three distinct relaxation regions in the time axis. The short-time dynamics follows $\exp(-kt^2)$ and stretched-exponential laws are found at long-time dynamics. As conjectured by Klafter and Shlesinger, this law arises from a scale-invariant distribution of relaxation times, which is only approximately fulfilled in the long-time limit, since the soft-core potential in general is not scale invariant. The breakdown of scale invariance is indicated by an oscillating feature in the relaxation between the short- and long-time limit.

For an inhomogeneously distributed (like Gaussian) sample, the ratio between the sample spatial size and the soft-core radius determines the degree of disorder of the system. In large Gaussian samples, strong disorder dominates and the dynamics shows similar behavior as the homogeneous case, while for small Gaussian samples a coherent many-body dynamics is found, since all spins interact pairwise with an almost constant interaction strength. A smooth change from the coherent regime to the strongly disordered one can be realized via tuning the Gaussian size of the sample. The ability to realize both fully ordered and strongly disordered spin systems in a single setting should be of high interest to experiments.

Our results in both homogeneous and inhomogeneous situations may stimulate experimental investigations in the cold-atom community and may also be generalized to other types of interaction potentials; a uniform gas can be prepared via the so-called box traps [40,41], and a Gaussian distribution of atoms is obtained with a harmonic trap [37].

ACKNOWLEDGMENTS

We are grateful to Xiaopeng Li for a careful reading of our manuscript, and T. Franz, G. Zürn, and S. Geier for discussions. We are supported by the Anhui Initiative in Quantum Information Technologies. Y.H.J. also acknowledges support from the National Natural Science Foundation under Grant No. 11827806. M.W. is supported by the Deutsche Forschungsgemeinschaft (DFG, German Research Foundation) under Germany's Excellence Strategy EXC2181/1-390900948 (the Heidelberg STRUCTURES Excellence Cluster), within the Collaborative Research Center SFB1225 (ISOQUANT) and the DFG Priority Program 1929 "GiRyd" (DFG WE2661/12-1).

APPENDIX

1. Analytic derivation in a homogeneous sample

To derive Eq. (8a) from $I(J_0t;\beta_0) = \int_{y_0}^{J_0t}(J_0t/y - 1)^{\beta_0}\sin y dy$ for $\beta_0 < 1$, we first introduce a new variable $x = 1/y$ in the later integral, resulting in

$$\begin{aligned}
I(J_0t;\beta_0) &= \int_{1/(J_0t)}^{1/y_0}(J_0tx-1)^{\beta_0}x^{-2}\sin(x^{-1})dx \quad \xrightarrow{y_0\to 0} \frac{(J_0t)^{\beta_0}}{2i}\int_{1/(J_0t)}^{\infty}\left(x-\frac{1}{J_0t}\right)^{\beta_0}x^{-2}(e^{ix^{-1}}-e^{-ix^{-1}})dx \\
&= \frac{(J_0t)^{\beta_0}}{2i}B(1-\beta_0,1+\beta_0)(J_0t)^{1-\beta_0}[{}_1F_1(1-\beta_0,2,iJ_0t) - {}_1F_1(1-\beta_0,2,-iJ_0t)] \\
&= J_0tB(1-\beta_0,1+\beta_0)\Im[{}_1F_1(1-\beta_0,2,iJ_0t)]. \qquad \text{(A1)}
\end{aligned}$$

Here we have used an integral formula listed in Ref. [42], which reads

$$\int_m^\infty x^{v-1}(x-m)^{\mu-1}e^{b/x}dx = B(1-\mu-v,\mu)m_1^{\mu+v-1}F_1(1-\mu-v,1-v,b/m) \qquad \text{(A2)}$$

and is valid for $m > 0, 0 < \Re(\mu) < \Re(1-v)$. $\Re(z)$ represents the real part of z. The asymptotic behavior of the Kummer confluent hypergeometric function ${}_1F_1(a,b,z)$ at large $|z|$ is ${}_1F_1(a,b,z) \sim \Gamma(b)[e^z z^{a-b}/\Gamma(a) + (-z)^{-a}/\Gamma(b-a)]$, which gives rise to Eq. (8c).

[1] K. Binder and A. P. Young, Rev. Mod. Phys. **58**, 801 (1986).
[2] C. A. Müller and D. Delande, *Les Houches Summer School Session XCI*, edited by C. Miniatura *et al.* (Oxford University Press, Oxford, UK, 2010).
[3] N. Upadhyaya and A. Amir, Phys. Rev. Materials **2**, 075201 (2018).
[4] E. J. Meier, F. A. An, A. Dauphin, M. Maffei, P. Massignan, T. L. Hughes, and B. Gadway, Science **362**, 929 (2018).
[5] S. Yu, C.-W. Qiu, Y. Chong, S. Torquato, and N. Park, Nat. Rev. Mater. **6**, 226 (2021).
[6] J. C. Phillips, Rep. Prog. Phys. **59**, 1133 (1996).

[7] J. Klafter and M. F. Shlesinger, Proc. Natl. Acad. Sci. **83**, 848 (1986).
[8] P. Schultzen, T. Franz, S. Geier, A. Salzinger, A. Tebben, C. Hainaut, G. Zürn, M. Weidemüller, and M. Gärttner, Phys. Rev. B **105**, L020201 (2022).
[9] W. Zhong, D. Panja, and G. T. Barkema, Phys. Rev. E **100**, 012132 (2019).
[10] A. Signoles, T. Franz, R. Ferracini Alves, M. Gärttner, S. Whitlock, G. Zürn, and M. Weidemüller, Phys. Rev. X **11**, 011011 (2021).
[11] P. Schultzen, T. Franz, C. Hainaut, S. Geier, A. Salzinger, A. Tebben, G. Zürn, M. Gärttner, and M. Weidemüller, arXiv:2107.13314.
[12] C. N. Likos, A. Lang, M. Watzlawek, and H. Löwen, Phys. Rev. E **63**, 031206 (2001).
[13] B. M. Mladek, D. Gottwald, G. Kahl, M. Neumann, and C. N. Likos, Phys. Rev. Lett. **96**, 045701 (2006).
[14] D. Coslovich, L. Strauss, and G. Kahl, Soft Matter **7**, 2127 (2011).
[15] F. Cinti, P. Jain, M. Boninsegni, A. Micheli, P. Zoller, and G. Pupillo, Phys. Rev. Lett. **105**, 135301 (2010).
[16] N. Henkel, R. Nath, and T. Pohl, Phys. Rev. Lett. **104**, 195302 (2010).
[17] M. Kunimi and Y. Kato, Phys. Rev. B **86**, 060510(R) (2012).
[18] P. Mason, C. Josserand, and S. Rica, Phys. Rev. Lett. **109**, 045301 (2012).
[19] F. Cinti, T. Macrì, W. Lechner, G. Pupillo, and T. Pohl, Nat. Commun. **5**, 3235 (2014).
[20] T. Macrì, S. Saccani, and F. Cinti, J. Low Temp. Phys. **177**, 59 (2014).
[21] S. Rossotti, M. Teruzzi, D. Pini, D. E. Galli, and G. Bertaina, Phys. Rev. Lett. **119**, 215301 (2017).
[22] S. Prestipino, A. Sergi, and E. Bruno, Phys. Rev. B **98**, 104104 (2018).
[23] S. Prestipino, A. Sergi, E. Bruno, and P. V. Giaquinta, EPJ Web Conf. **230**, 00008 (2020).
[24] F. Mambretti, S. Molinelli, D. Pini, G. Bertaina, and D. E. Galli, Phys. Rev. E **102**, 042134 (2020).
[25] Y.-Y. Jau, A. M. Hankin, T. Keating, I. H. Deutsch, and G. W. Biedermann, Nat. Phys. **12**, 71 (2016).
[26] J. Zeiher, R. van Bijnen, P. Schauß, S. Hild, J.-y. Choi, T. Pohl, I. Bloch, and C. Gross, Nat. Phys. **12**, 1095 (2016).
[27] J. Zeiher, J.-y. Choi, A. Rubio-Abadal, T. Pohl, R. van Bijnen, I. Bloch, and C. Gross, Phys. Rev. X **7**, 041063 (2017).
[28] V. Borish, O. Marković, J. A. Hines, S. V. Rajagopal, and M. Schleier-Smith, Phys. Rev. Lett. **124**, 063601 (2020).
[29] S. Hollerith, K. Srakaew, D. Wei, A. Rubio-Abadal, D. Adler, P. Weckesser, A. Kruckenhauser, V. Walther, R. van Bijnen, J. Rui *et al.*, Phys. Rev. Lett. **128**, 113602 (2022).
[30] L. I. R. Gil, R. Mukherjee, E. M. Bridge, M. P. A. Jones, and T. Pohl, Phys. Rev. Lett. **112**, 103601 (2014).
[31] A. W. Glaetzle, M. Dalmonte, R. Nath, I. Rousochatzakis, R. Moessner, and P. Zoller, Phys. Rev. X **4**, 041037 (2014).
[32] A. W. Glaetzle, M. Dalmonte, R. Nath, C. Gross, I. Bloch, and P. Zoller, Phys. Rev. Lett. **114**, 173002 (2015).
[33] R. M. W. van Bijnen and T. Pohl, Phys. Rev. Lett. **114**, 243002 (2015).
[34] A. Glicenstein, G. Ferioli, L. Brossard, Y. R. P. Sortais, D. Barredo, F. Nogrette, I. Ferrier-Barbut, and A. Browaeys, Phys. Rev. A **103**, 043301 (2021).
[35] G. G. Emch, J. Math. Phys. **7**, 1198 (1966).
[36] C. Radin, J. Math. Phys. **11**, 2945 (1970).
[37] W. Ketterle, D. S. Durfee, and D. M. Stamper-Kurn, arXiv:cond-mat/9904034.
[38] J. Schachenmayer, A. Pikovski, and A. M. Rey, Phys. Rev. X **5**, 011022 (2015).
[39] J. G. Bohnet, B. C. Sawyer, J. W. Britton, M. L. Wall, A. M. Rey, M. Foss-Feig, and J. J. Bollinger, Science **352**, 1297 (2016).
[40] A. L. Gaunt, T. F. Schmidutz, I. Gotlibovych, R. P. Smith, and Z. Hadzibabic, Phys. Rev. Lett. **110**, 200406 (2013).
[41] B. Mukherjee, Z. Yan, P. B. Patel, Z. Hadzibabic, T. Yefsah, J. Struck, and M. W. Zwierlein, Phys. Rev. Lett. **118**, 123401 (2017).
[42] I. S. Gradshteį n and D. Zwillinger, *Table of Integrals, Series, and Products*, 8th ed. (Elsevier, Academic Press, 2015).